

Difference Methods for the Piston Problem

By

Tatsuo NOGI*

(Received November 12, 1968)

We shall consider a piston problem in hydrodynamics and give difference methods to solve it.

Our aim is to find the algorithm in the neighbourhood of the piston in which the piston motion is calculated simultaneously. In our experiment we shall use the modified Godunov's scheme in the interior region away from the piston. Our method is an extension of the scheme to the boundary value problem.

1. Introduction

We consider the piston problem¹⁾ in hydrodynamics which arise from some models of gun-tunnels,³⁾ free piston shock tubes,²⁾ etc.. This problem has been difficult to be solved analytically, while for the design of the above apparatuses we have several approximation techniques which use mainly characteristics and shock conditions, so that they seem to be very inconvenient. Then we have arrived at the necessity of direct algorithm solving the equation of hydrodynamics by difference methods.

In view of the studies of difference schemes themselves many authors have attacked the Cauchy problem, while for mixed initial-boundary value problems, we know only a few results and we are not in the position having any practically effective methods. Here we aim to discover an appropriate method for mixed problems.

As a simple one-dimensional model of a gun-tunnel we take the following system.

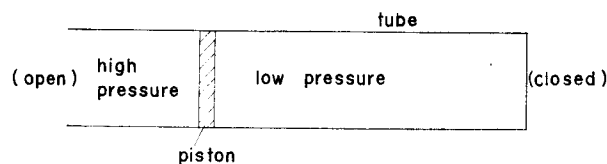


Fig. 1. The model of the gun-tunnel.

* Department of Applied Mathematics and Physics

Here the cross area of the tube is assumed to be constant, initially the piston is positioned at some point and the states of gas in the both chambers rest uniformly, and the pressure of the gas in the left chamber is higher than that in the right chamber. As soon as the piston is set free it begins to move by difference of the forces acting on both sides of the piston. Our aim is to introduce an algorithm to solve it numerically.

The algorithm is mainly depending on Godunov's idea¹⁾ and is constructed to calculate also in the neighborhood of boundary points.

2. Differential Equations and Boundary Conditions

Mainly we shall use the usual equation of hydrodynamics in the Eulerian form and the polytropic relation to express the motion and state of gas in each chamber:

$$(2.1) \quad \begin{aligned} \rho_t + (\rho u)_x &= 0 \\ (\rho u)_t + (p + \rho u^2)_x &= 0 \\ \left\{ \rho \left(e + \frac{1}{2} u^2 \right) \right\}_t + \left\{ \rho u \left(e + \frac{1}{2} u^2 + \frac{p}{\rho} \right) \right\}_x &= 0 \\ p &= (\gamma - 1) \rho e \end{aligned}$$

where ρ is the density, u is the velocity, p is the pressure, e is the internal energy per unit mass and γ is the adiabatic exponent.

The equation of the piston motion is as following:

$$(2.2) \quad \frac{d^2 \xi(t)}{dt^2} = p(t, \xi(t) - 0) - p(t, \xi(t) + 0), \quad \xi(0) = 0$$

where $x = \xi(t)$ is the piston path, and we can assume by appropriately normalizing that the piston mass is unit.

The boundary condition being satisfied at the position of the piston is

$$u(t, \xi(t) - 0) = u(t, \xi(t) + 0) = \frac{d\xi(t)}{dt}.$$

Furthermore we have the following boundary condition at the right end wall ($x = x_w$):

$$u(t, x_w) = 0.$$

As initial conditions we suppose that the initial static states have uniformly constant density and pressure in each chamber.

3. The Modified Godunov's Scheme

For solving the above problem we must make up algorithms in the neighborhood of the piston, in that of the wall and through the inner region respectively.

First we consider the scheme through the inner region.

One wants such schemes as reproduce especially shock waves which are discontinuous solutions. Such schemes, as far as we know, are divided into two classes. One is of the method using "artificial viscosity" and the other depends on "the decay of the discontinuity". An example of the former is the Lax-Wendroff's scheme^{5),7)} and that of the latter is the Godunov's scheme⁴⁾. Both are known to be excellent methods, but according to our experiments for the Riemann problem it seemed that the modified Godunov's scheme⁶⁾ is a little better than the L-W⁷⁾ scheme, and we shall use mainly the modified Godunov's scheme.

Now we will show briefly the Godunov's scheme and the modified one. On a time level we consider the grid function as the step function having discontinuities at the half-integer points. First we shall solve the decay of the discontinuities and secondly calculate the mean values around each grid point on the next time step. So formed grid functions are used to take the next step, and so on.

In order to proceed to such an algorithm we had better use the following integral formula instead of the original differential equations (2.1):

$$\begin{aligned}
 \oint \rho dx - \rho u dt &= 0 \\
 \oint \rho u dx - (p + \rho u^2) dt &= 0 \\
 \oint \rho \left(e + \frac{u^2}{2} \right) dx - \rho u \left(e + \frac{u^2}{2} + \frac{p}{\rho} \right) dt &= 0
 \end{aligned}
 \tag{3.1}$$

In the Fig-2 we want to know the unknown value at the grid point A. Then we take the integral contour CEFD. For example, we have for the first equation of (3.1)

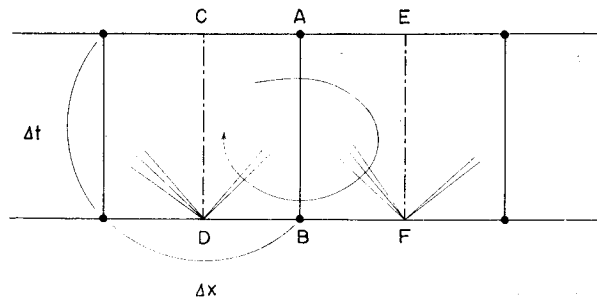


Fig. 2.

$$(3.2) \quad \Delta x \bar{\rho}_A = \Delta x \bar{\rho}_B - \Delta t \{ (\overline{\rho u})_{FE} - (\overline{\rho u})_{CD} \},$$

so that we can know the mean value $\bar{\rho}_A$ around the grid point A if we know ρu 's on the lines EF and CD, which are obtained by solving the decay of discontinuities at F, D respectively. For solving the decay of discontinuities we must go through an iteration process. In order to avoid it we shall use below the modified Godunov's scheme, in which the waves are supposed to propagate to right and left along characteristics. This assumption is valid only for the case in which quantities of jump are small. Thus we have the following algorithm:

$$(3.3) \quad \begin{aligned} \rho^j &= \rho_j \lambda_j (R_{j+1/2} U_{j+1/2} - R_{j-1/2} U_{j-1/2}) \\ \rho^j u^j &= \rho_j u_j - \lambda (P_{j+1/2} + R_{j+1/2} U_{j+1/2}^2 - P_{j-1/2} - R_{j-1/2} U_{j-1/2}^2) \\ \rho^j \left(e^j + \frac{1}{2} (u^j)^2 \right) &= \rho_j \left(e_j + \frac{1}{2} u_j^2 \right) \\ &\quad - \lambda \left\{ R_{j+1/2} U_{j+1/2} \left(E_{j+1/2} + \frac{1}{2} U_{j+1/2}^2 + \frac{P_{j+1/2}}{R_{j+1/2}} \right) \right. \\ &\quad \left. - R_{j-1/2} U_{j-1/2} \left(E_{j-1/2} + \frac{1}{2} U_{j-1/2}^2 + \frac{P_{j-1/2}}{R_{j-1/2}} \right) \right\} \\ \rho^j &= (\tau - 1) \rho^j e^j \quad \lambda = \frac{\Delta t}{\Delta x} \end{aligned}$$

where the lower suffix indicates the x -position on a time level $t=t_0$, and the upper indicates ones on $t=t_0 + \Delta t$.

The auxiliary values are calculated as follows:

$$\begin{aligned} a_{j+1/2} &= \sqrt{\tau \frac{\rho_j + \rho_{j+1}}{2} \frac{\rho_j + \rho_{j+1}}{2}} \\ \rho_{j+1/2} &= \frac{\rho_{j+1} + \rho_j}{2} - a_{j+1/2} \frac{u_{j+1} - u_j}{2} \\ u_{j+1/2} &= \frac{u_{j+1} + u_j}{2} - \frac{\rho_{j+1} - \rho_j}{2a_{j+1/2}} \\ \rho_{j+1/2}^L &= \frac{(\tau + 1)\rho_{j+1/2} + (\tau - 1)\rho_j}{(\tau - 1)\rho_{j+1/2} + (\tau + 1)\rho_j} \rho_j \\ \rho_{j+1/2}^R &= \frac{(\tau - 1)\rho_{j+1/2} + (\tau - 1)\rho_{j+1}}{(\tau + 1)\rho_{j+1/2} + (\tau + 1)\rho_{j+1}} \rho_{j+1} \\ S_{j+1/2}^L &= u_j - \frac{a_{j+1/2}}{\rho_j}, \quad S_{j+1/2}^R = u_{j+1} + \frac{a_{j+1/2}}{\rho_{j+1}} \end{aligned}$$

Consequently we have the following four cases for large capitals U, P, R and E:

i) If $S_{j+1/2}^L > 0$, $S_{j+1/2}^R > 0$, then

$$U_{j+1/2} = u_j, \quad P_{j+1/2} = p_j, \quad R_{j+1/2} = \rho_j$$

ii) If $S_{j+1/2}^L < 0, S_{j+1/2}^R < 0$, then

$$U_{j+1/2} = u_{j+1}, \quad P_{j+1/2} = p_{j+1}, \quad R_{j+1/2} = \rho_{j+1}$$

iii) If $S_{j+1/2}^L < 0, S_{j+1/2}^R > 0, u_{j+1/2} > 0$, then

$$U_{j+1/2} = u_{j+1/2}, \quad P_{j+1/2} = p_{j+1/2}, \quad R_{j+1/2} = \rho_{j+1/2}^L$$

iv) If $S_{j+1/2}^L < 0, S_{j+1/2}^R > 0, u_{j+1/2} < 0$, then

$$U_{j+1/2} = u_{j+1/2}, \quad P_{j+1/2} = p_{j+1/2}, \quad R_{j+1/2} = \rho_{j+1/2}^R$$

$$\text{and } E_{j+1/2} = \frac{P_{j+1/2}}{(r-1)R_{j+1/2}}$$

By the linear stability analysis it is known that this scheme is stable under the C.F.L. condition.

4. The Algorithm in the Neighbourhood of the Piston

Next we consider the neighbourhood of the piston. Since the piston moves across the net, the algorithm becomes complicated. In order to compare quantitatively the various methods, we had the numerical experiments of the piston problem for the linear wave equation in which the piston was to be moved with constant acceleration. And we have arrived at the method having the comparatively small errors (see Appendix-1). This method can be also applied to the nonlinear equation of the fluid dynamics. In our experiment this method gave good results (see Appendix-II). Here we are to interpret the method when the piston moves to the right, the piston path are drawn on the net in the following two ways for sufficiently small Δt . (Fig. 3)

In the Fig. 3-a,b we suppose that the values of u, ρ, p at the mesh points mesh points A,B,C,D etc. and that at the point P of the piston are known. Then we desire those values at the points A', B', C', D', and P' after Δt . For this we

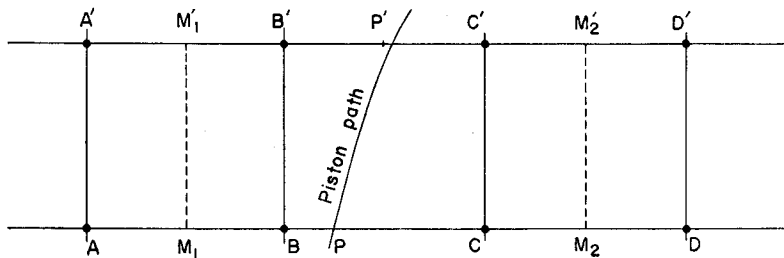


Fig. 3-a.

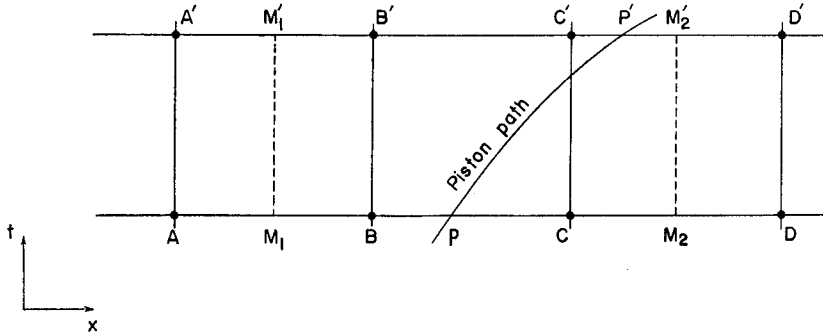


Fig. 3-b.

again use the integral formulas (3.1). If we integrate along the contour $P'M_2'M_2P$ in the Fig. 3-a, we can have the integrated values (consequently the mean values) on the $P'M_2'$ using the integrated values on the $M_2'M_2$, M_2P and PP' . Therefore we shall first calculate the mean values on the $M_2'M_2$ and PP' . Supposing that the mean values are kept constant on the PM_2 and that the piston runs along PP' with a known positive constant speed we can decide the state in front of the piston by using the Rankine-Hugoniot's relation across the shock wave generated at the point P ; we find first the shock speed U

$$U = \frac{1}{2} \frac{\bar{u}_p - \bar{u}}{1 - \mu^2} + \sqrt{\bar{c}^2 + \frac{1}{4} \left(\frac{\bar{u}_p - \bar{u}}{1 - \mu^2} \right)^2} \quad \mu^2 = \frac{\gamma - 1}{\gamma + 1}$$

where \bar{u}_p is the piston speed (the suffix p and the bar means here and just below the mean values on the PP' and "+"-in front of, "-"-at the back of) and the barred values \bar{u} and \bar{c} means the mean values on the PM_2 of the velocity and the sound velocity respectively (the bars mean here and below the mean values on the PM_2) and furthermore we find

$$(4.1) \quad \begin{aligned} \bar{p}_+ &= \bar{p} \left\{ (1 + \mu^2) \frac{(U - \bar{u})^2}{\bar{c}^2} - \mu^2 \right\} \\ \bar{\rho}_+ &= \bar{\rho} \frac{\bar{p}_+ + \mu^2 \bar{p}}{\bar{p} + \mu^2 \bar{p}_+} \end{aligned}$$

The desired values on the $M_2'M_2$ are calculated by the decay of the discontinuity at the point M_2 as we have done above in the interior region. Hereafter we have the mean values $\bar{\sim}$ on the $P'M_2'$ as follow:

$$(4.2) \quad \begin{aligned} \bar{p} &= \alpha \bar{\rho} - \beta (\rho u)_{M_2 M_2'} \\ \bar{\rho} &= \alpha \bar{\rho} u - \beta \{ (\bar{p} + \rho u^2)_{M_2 M_2'} - \bar{p}_p \} \\ \bar{\rho} \left(e + \frac{u^2}{2} \right) &= \alpha \bar{\rho} \left(e + \frac{u^2}{2} \right) - \beta \left[\left(\rho u \left(e + \frac{u^2}{2} + \frac{\bar{p}}{\rho} \right) \right)_{M_2 M_2'} - (\bar{p} u)_p \right] \end{aligned}$$

where $\alpha = \overline{PM_2} / \overline{P'M_2'}$, $\beta = \Delta t / \overline{P'M_2'}$ and $(\cdot)_{M_2M_2'}$ indicates the mean values on the M_2M_2' . On the other hand under the same hypothesis of the piston motion the expansion wave propagates backward.

We can also decide the state at the back of the piston as follows:

$$(4.3) \quad \begin{aligned} \bar{p}_- &= \bar{p} \left[1 - \frac{\gamma-1}{2} \frac{u_p - \bar{u}}{\bar{c}} \right]^{2\gamma/(\gamma-1)} \\ \bar{\rho}_- &= \bar{\rho} \left[1 - \frac{\gamma-1}{2} \frac{u_p - \bar{u}}{\bar{c}} \right]^{2/(\gamma-1)} \end{aligned}$$

where the doubly-barred values show the mean values on the M_1P . The desired mean values on the $M_2'P'$ are calculated by using again the integral formulas (3.1) along the path $M_1'P'PM_1$. Contrarily when the piston moves with a known negative constant speed, we have the shock wave to the left and the expansion wave to the right. Then we can calculate the mean values on the $M_1'P'$ and $P'M_2'$ in similar way. While in the case of the Fig. 3-b, we shall decide the states the front of and at the back of the piston just in the same way as in the case of Fig. 3-a, the values at the point D' are calculated by the interior formula. Thus we have the mean values in the neighbourhood of the piston, and furthermore we can calculate the desired values at the grid points by the interpolation between the corresponding mean values and the states at the piston.

So far we supposed that the piston speed was to be known in advance, but in reality it is unknown beforehand and is the quantity to be desired. If we know the states at both sides of the piston, we can know the piston speed by integrating the equation of the piston motion. Approximately we have the following the formula:

$$(4.4) \quad \begin{aligned} u_p' &= u_p + \Delta t (\bar{p}_- - \bar{p}_+) \\ u_p &= \frac{u_p' + u_p}{2} \end{aligned}$$

Hence in order to know the states of both sides at the piston and the speed of the piston, we can not but use the iteration scheme among the formulas (4.1), (4.3) and (4.4). It is easily seen that this iteration scheme converges for small Δt .

5. The Algorithm in Front of the Wall

We suppose that the net is set in front of the wall as Fig. 4,

We shall construct the scheme which gives the relevant values at the mesh point E' and at the point \bar{W} on the wall using the values at E and F etc.. For this along the same line as in the neighbourhood of the piston we consider the reflection of

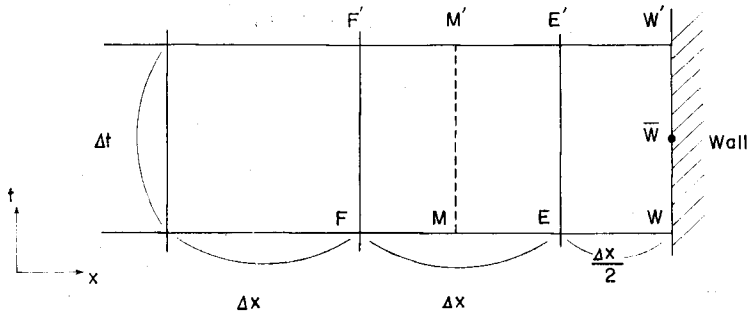


Fig. 4.

the shock wave at the point W on the wall and ask the state on the wall using the Rankine-Hugoniot relation, and furthermore apply the contour-integral (3.1) along $M'W'WM$ so that we have the relevant values at the mesh point E' . Here, of course, it is supposed that we have a uniform state along MW and we calculate the decay of the discontinuity at the point M as in the interior region. Consequently this algorithm is put in order as follows:

$$c_E = \sqrt{\frac{\gamma p_E}{\rho_E}}$$

$$u_S = -\frac{u_E}{2(1-\mu^2)} - \sqrt{c_E^2 + \left(\frac{u_E}{2(1-\mu^2)}\right)^2}$$

$$p_{\bar{W}} = p_E \left\{ (1+\mu^2) \left(\frac{u_S}{c_E}\right)^2 - \mu^2 \right\}$$

$$\rho_{\bar{W}} = \frac{\gamma p_{\bar{W}}}{c_E^2 - \frac{\gamma-1}{2} u_E (2u_S + u_E)}$$

6. An Experiment

In order to check our method we use the following data as an example: the length of the barrel between the initial position and the closed end is 3.5 m, the radius is 3.7 cm, the pressure in the barrel (the right chamber) is 2.8 kg W/cm², that in the reservoir (the left chamber) is 66 kg W/cm², the initial sound velocity in both chambers is 331 m/sec and the piston weight W is 0.005 kgW. These data depend on that of the hypersonic gun tunnel at the Kyoto University constructed in 1962³⁾. We carry out, as usual, to nondimensionalize as follows:

$$u \rightarrow \bar{u} = \frac{u}{c_0} \quad c_0^2 = \frac{\gamma p_0}{\rho_0}$$

$$p \rightarrow \bar{p} = \frac{p}{p_0} \quad \rho \rightarrow \bar{\rho} = \tau \frac{\rho}{\rho_0}$$

$$x \rightarrow \bar{x} = \frac{gp_0 A_0 x}{W \cdot c_0^2}, \quad t \rightarrow \bar{t} = \frac{gp_0 A_0 t_0}{W c_0}$$

where W is the piston weight, A_0 is the cross area of the barrel and g is the gravitational acceleration.

The zero suffix of the other values means the initial values in the right chamber. Thus we have the equations of hydrodynamics (2.1) and the equation of the piston motion (2.2), where the bar is omitted. And the above initial data are reduced to the following non-dimensional quantities;

$$p_0 = 1 \quad \rho_0 = 1.4 \quad u_0 = 0 \quad (\text{in the right chamber})$$

$$p_1 = 23.57 \quad \rho_1 = 13.37 \quad u_1 = 0 \quad (\text{in the left chamber})$$

and the length of the barrel is 1.88.

In our experiments $\Delta x = 0.094$, $\lambda = 0.2$ which satisfies the C.F.L. condition⁷⁾ in our data and results. In Fig. 5 we see how the pressure in the chambers varies as time passes. In the Fig. 6 we see the piston path (the real line) and the aspect of the propagation of the shock waves. The pressure at the end wall varies as in Fig. 7. This pattern agrees fairly with the experimental result.³⁾

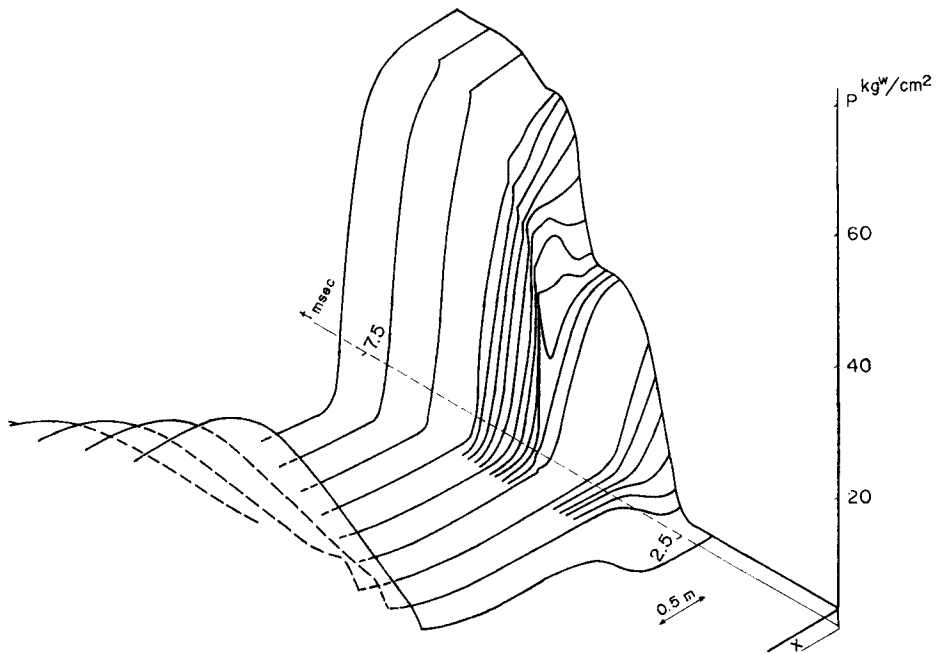


Fig. 5. The pressure history.

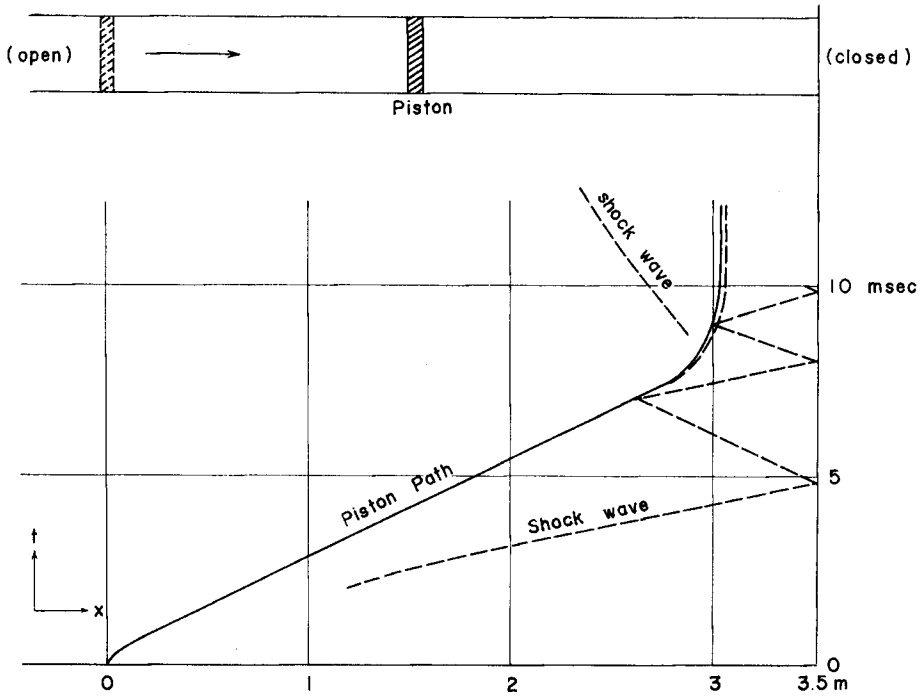


Fig. 6. The piston path (the real line-by the Eulerian formula, the broken line-by the Lagrangian formula) and the propagation of the shock wave.

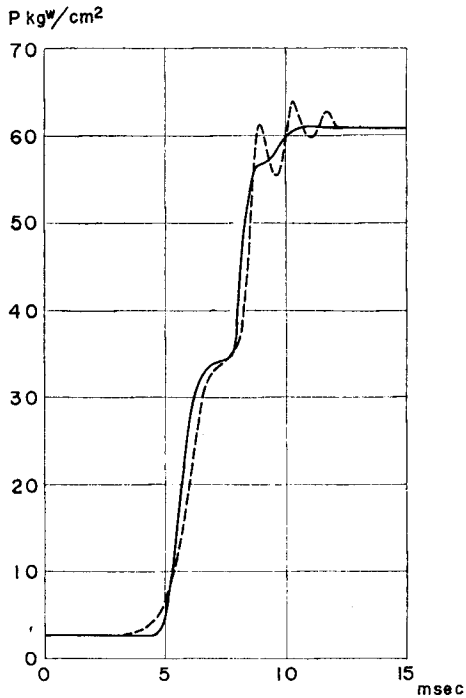


Fig. 7. The pressure history at the wall (the real line-by the Eulerian formula, the broken line-by the Lagrangian formula).

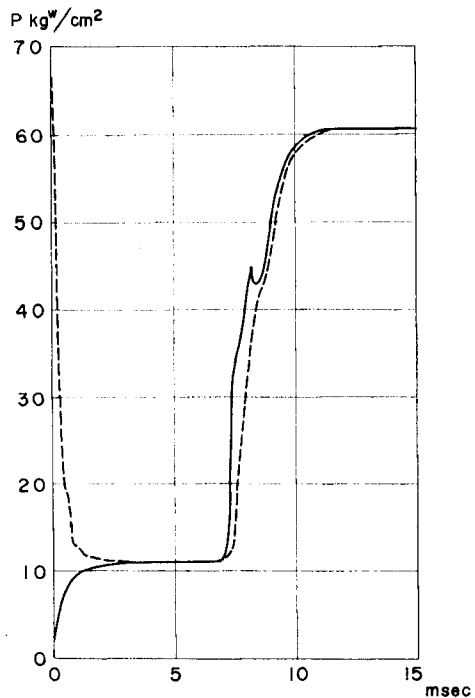


Fig. 8. The pressure histories in the front of (the real line) and at the back of the piston (the broken line).

Futhermore the pressure histories in the front of the piston (the solid line) and at the back of (the broken line) are shown in Fig. 8. In order to check our result we shall compute the theoretical pressure and the one of our numerical experiment at the back of the forward shock wave while the piston runs with constant speed. The former was 3.94 (with no dimension) and the latter was 3.96.

Appendix I

We shall consider the piston problem for the wave equation

$$(I-1_1) \quad \begin{cases} u_t = v_t \\ v_t = u_x, \end{cases} \quad x > X(t), \quad t > 0.$$

Initial conditions:

$$(I-1_2) \quad u(0, x) = 0, \quad v(0, x) = 1.0, \quad x > 0$$

Piston path:

$$(I-1_3) \quad X(t) = 0.1t^2$$

Boundary condition:

$$(I-1_4) \quad u|_{x=X(t)} = 0.2t$$

And we shall try to compare the various algorithms in the neighbourhood of the piston.

We shall approximate the differential equation by the following difference equation (the Godunov's scheme):

$$(I-2) \quad \begin{aligned} u_j^{n+1} &= u_j^n + \frac{\lambda}{2} (v_{j+1}^n - v_{j-1}^n) + \frac{\lambda}{2} (u_{j+1}^n - 2u_j^n + u_{j-1}^n) \\ v_j^{n+1} &= v_j^n + \frac{\lambda}{2} (u_{j+1}^n - u_{j-1}^n) + \frac{\lambda}{2} (v_{j+1}^n - 2v_j^n + v_{j-1}^n) \end{aligned}$$

Now when the net is fixed, the piston path runs across it in the following two ways:

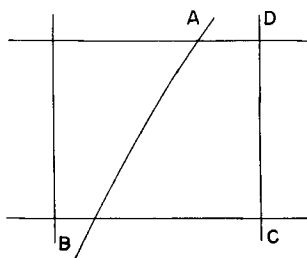


Fig. 9-a.

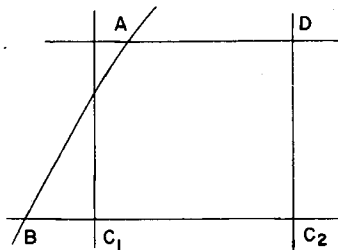


Fig. 9-b.

The problem is to determine the relevant values at the points A and D using those at the point B, C, etc.,

(i) Method-1 First we shall introduce the most formal method. In the case-a

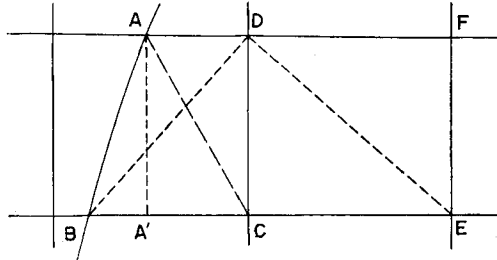


Fig. 10-a.

We shall put

$$BA' : A'C = \alpha : \beta \quad BC : CE = \alpha' : \beta'$$

$$(\alpha + \beta = \alpha' + \beta' = 1)$$

and

$$v_A = \alpha v_C + \beta v_B + \frac{\Delta t}{BC} (u_C - u_B)$$

$$u_D = \alpha' u_E + \beta' u_B + \frac{\Delta t}{BE} (v_E - v_B)$$

$$v_D = \alpha' v_E + \beta' v_B + \frac{\Delta t}{BE} (u_E - u_B)$$

In the case-b

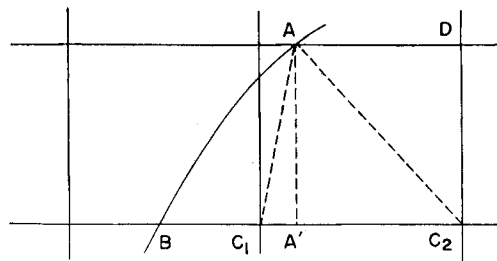


Fig. 10-b.

We shall put

$$C_1A' : A'C_2 = \alpha : \beta \quad (\alpha + \beta = 1)$$

and

$$v_A = \alpha v_{C_2} + \beta v_{C_1} + \lambda (u_{C_2} - u_{C_1}) \quad \left(\lambda = \frac{\Delta t}{\Delta x} \right)$$

The relevant values at D are calculated by the formula (I-2)

The experiment by this method is shown in Fig. 11, where $\lambda=1.0$, $\Delta x=0.2$ and the parameter on the curve means the time.

The broken line shows the exact solution of the problem (I-1). (These conventions are common among the following figures.)

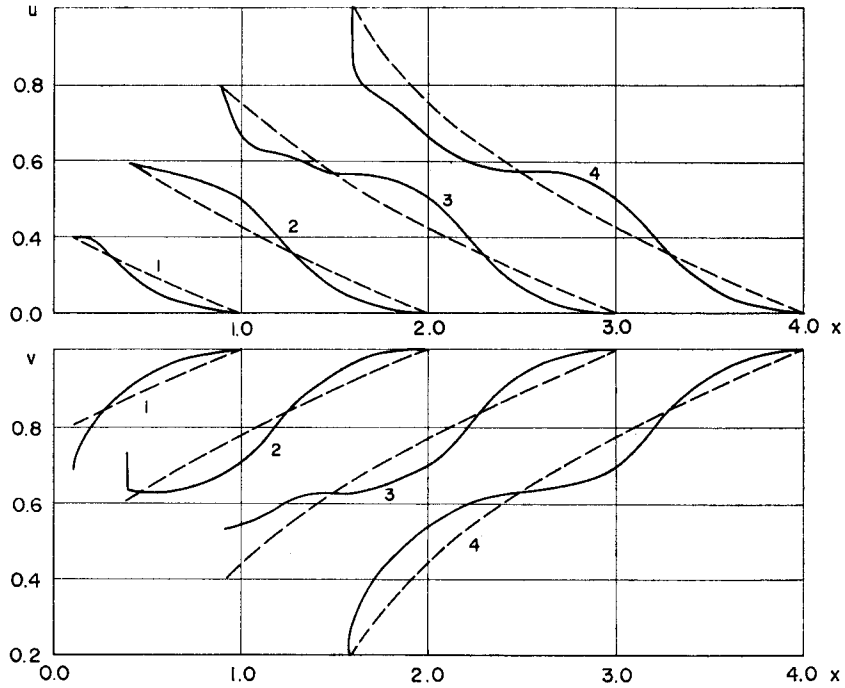


Fig. 11. Method-1.

(ii) Method-2 In the result by the Method-1 the values at the piston become far from the exact ones and its effects are propagated to the right. In order to determine the values better we shall use the characteristics, that is, use the property of the solution that $u+v$ remain constant along the line $\frac{dx}{dt} = -1$.

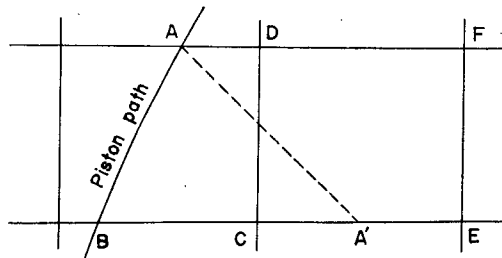


Fig. 12.

Draw the characteristic AA' ($\frac{dx}{dt} = -1$) through the point A and determine the position A' as Fig. 12 and set

$$v_A + u_A = v_{A'} + u_{A'}$$

If we determine the values $v_{A'}$ and $u_{A'}$ by interpolation between C and E, we have the value v_A (u_A is given).

The method to determine the values at the point D is as Method-1. By this algorithm we have the experimental results in Fig. 13. This result is certainly better than that of Method-1 and shows the aspect of the exact solution nearly in spite of the coarse mesh width $\Delta x = 0.2$. A defect is, as we see in the Fig. 13, the notable difference of the values at A, D when D is close to A. This means defect of the way calculating the value at D.

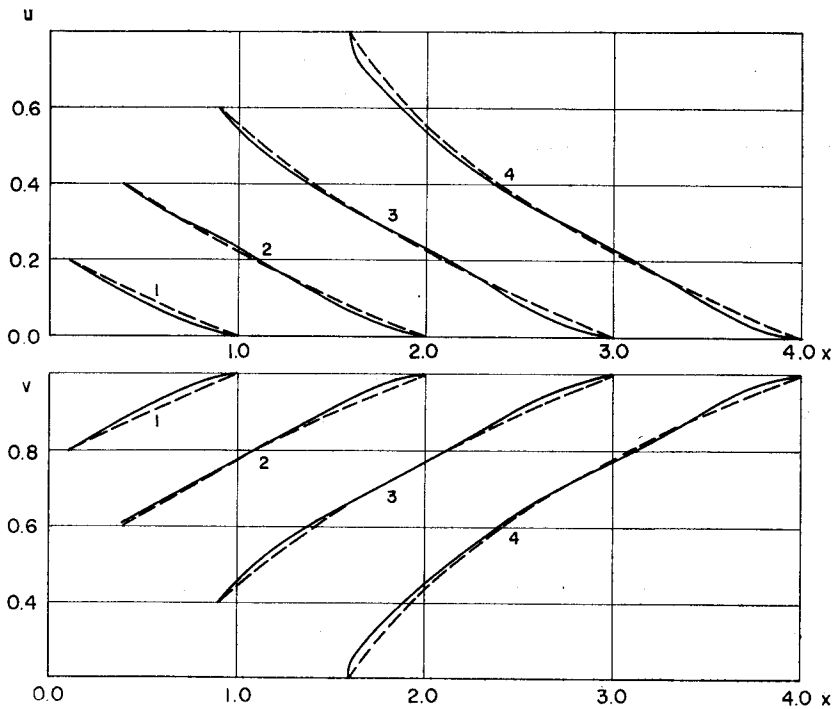


Fig. 13. Method-2.

(iii) Method-3 Another defect of Method II is that when it is applied to fluid dynamics, we must repeat the iteration process (even in the case where the piston motion is known in advance) to determine the relevant values at A.

Here we consider the way which does not use the characteristics as above.

It depends on the idea of "decay of discontinuity" and "integral formula", by which Godunov's scheme also was constructed in the internal region.

First we write the integral formula for (I-1),

$$(I-3) \quad \oint u dx + v dt = 0$$

$$\oint v dx + u dt = 0$$

Hence we have the jump condition

$$[u]s + [v] = 0$$

$$[v]s + [u] = 0$$

i.e.

$$(I-4) \quad s = \pm 1, \quad [u] = \pm [v]$$

where s is the slope of the discontinuity line, and $[\cdot]$ means the quantity of the jump. In this case the discontinuity line coincides with the characteristics.

We consider the case a and b:

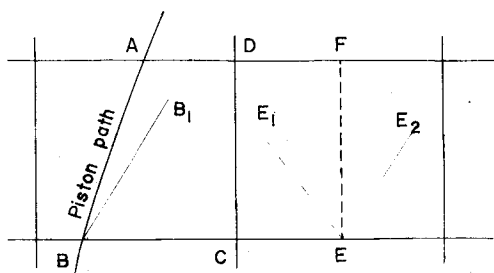


Fig. 14-a.

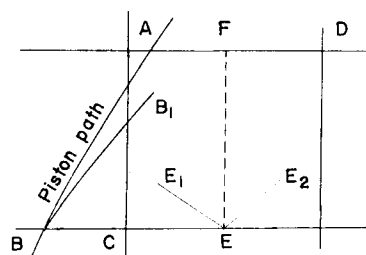


Fig. 14-b.

In both states we consider that the integral mean values $\overline{u_{BE}}$, $\overline{v_{BE}}$ are kept constant between B and E, and that the mean value $u_M = \frac{1}{2}(u_A + u_B)$, $v_M = \frac{1}{2}(v_A + v_B)$ are kept constant between A and B. Then the discontinuity line BB_1 ($s=1$) is generated from the point B and along it we have by the jump condition (I-4)

$$u_M + v_M = \overline{v_{BE}} + \overline{u_{BE}}.$$

From this formula v_M , and thus v_A are determined.

In the case-a we take the integral path ABEFA and write down (I-3) in order to determine the state of D,

$$\bar{u}AF = \bar{u}_{BE} \bar{BE} + \{V_E - (u_M^2 + v_M)\} \Delta t$$

$$\bar{v}AF = \bar{v}_{BE} \bar{BE} + \{U_E - (u_M v_M + u_M)\} \Delta t$$

where \bar{AF} and \bar{BE} mean the lengths of the intervals AF and BE respectively. The large characters U_E and V_E mean the states in the region $E_1 EE_2$ which are produced by the decay of the discontinuity at the point E. \bar{u} and \bar{v} are the mean values between A and F. Considering them as the value at the middle point of AF, we can calculate ones at D using also the values at A by interpolation or extrapolation. In the case-b, the values at D are determined by (I-2). The experimental result by the method is shown in Fig. 15 and is very good.

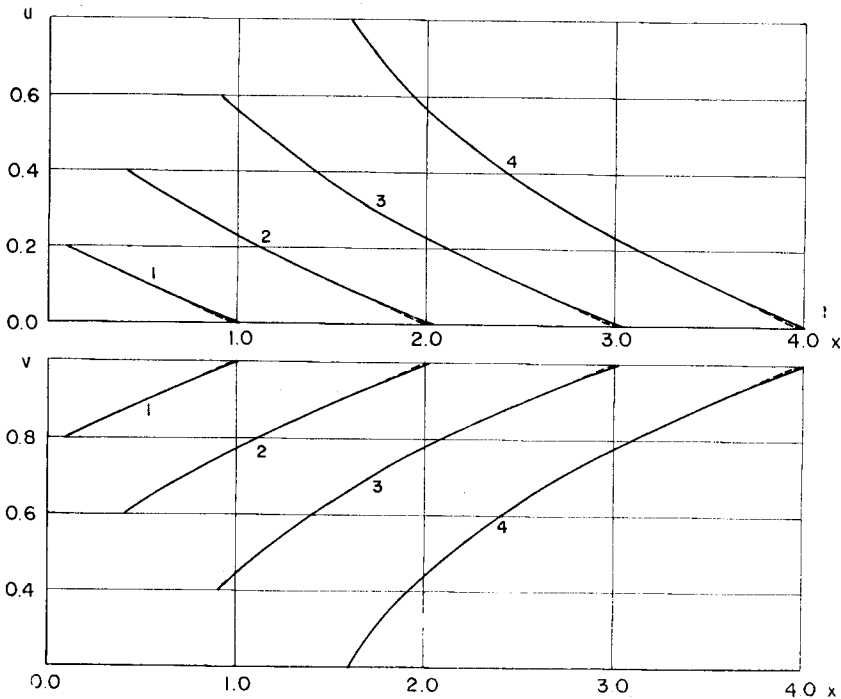


Fig. 15. Method-3.

In order to compare the above three methods we calculated the sum ϵ of the absolute value of the differences between the exact solution and the numerical at mesh points in the right of the piston on each line $t = \text{const}$. These errors are shown in Fig. 16.

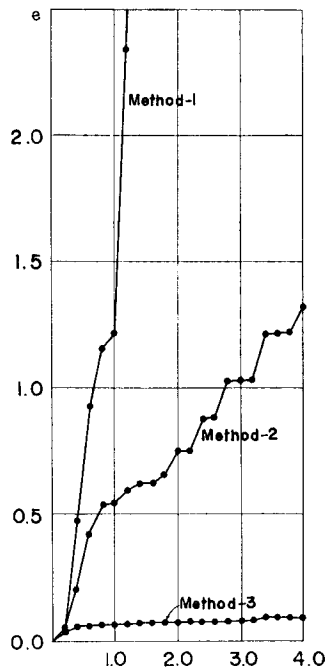


Fig. 16. The evolution of the errors.

Appendix II

Here we shall report the numerical experiments for the equation of fluid dynamics (2.1) in which the constant accelerated piston motion (on the half way, and then constant-speed-motion) is treated by several methods. The piston path is given by the equation

$$x = \xi(t) = \begin{cases} \frac{1}{2}t^2 & 0 \leq t \leq 1 \\ t - \frac{1}{2} & 1 \leq t. \end{cases}$$

Initial conditions are

$$u(0, x) = 0, \quad \rho(0, x) = 10.0 \quad p(0, x) = 2.0.$$

(i) Method-1 We shall again consider two cases:

In both cases we use the formulas, for example,

$$\begin{aligned} \frac{\rho_A - \rho_{A'}}{\Delta t} + \frac{(\rho u)_C - (\rho u)_B}{\overline{BC}} = 0 & \quad \rho_{A'} = \frac{\overline{BA'} \rho_C + \overline{A'C} \rho_B}{\overline{BC}} \\ \frac{\rho_D - \tilde{\rho}_C}{\Delta t} + \frac{(\rho u)_E - (\rho u)_B}{\overline{BE}} = 0 & \quad \tilde{\rho}_C = \frac{\overline{BC} \cdot \rho_E + \overline{CE} \cdot \rho_B}{\overline{BE}} \end{aligned}$$

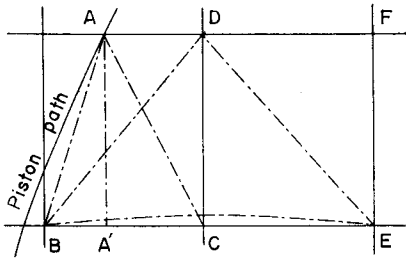


Fig. 17-a.

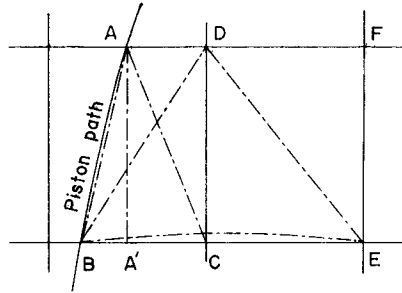


Fig. 17-b.

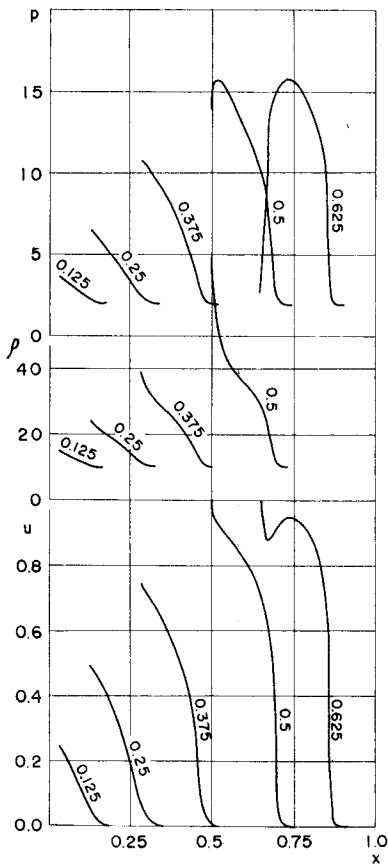


Fig. 18. Method-1.

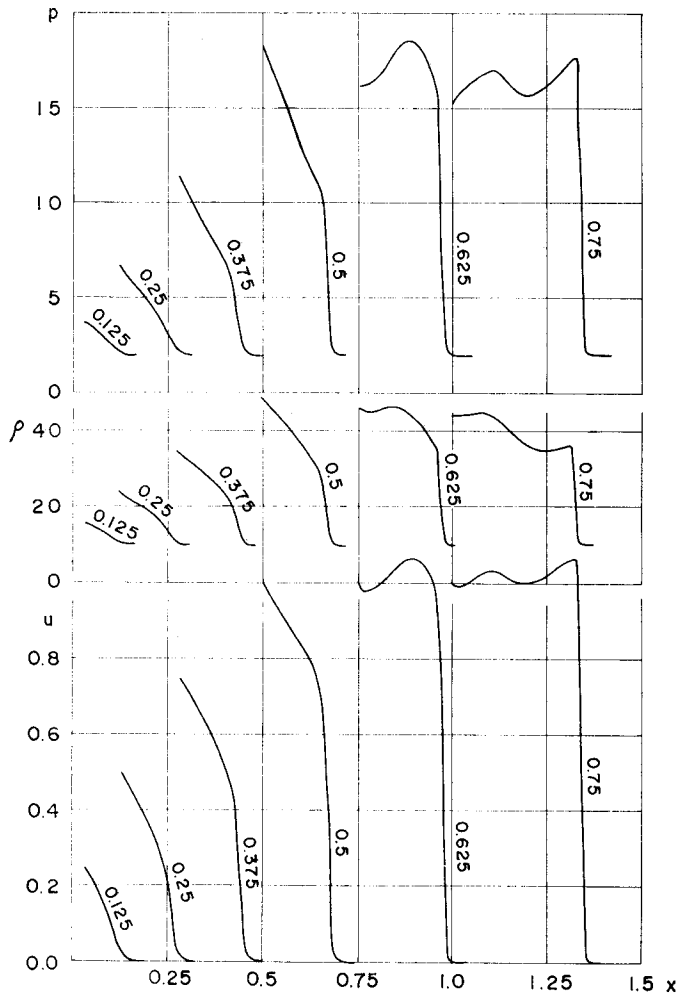


Fig. 19. Method-2.

Analogous construction is done for the rest equations.

The numerical result by this method is shown in the Fig. 18.

(ii) Method-2. Instead of the last equation in the Method-1 we use the following formula,

$$\frac{\rho_D - \rho_C}{\Delta t} + \frac{(\rho u)_E - (\rho u)_B}{BE} = 0,$$

see the Fig. 19

(iii) Method-3 This method is that of §2. Here we have put

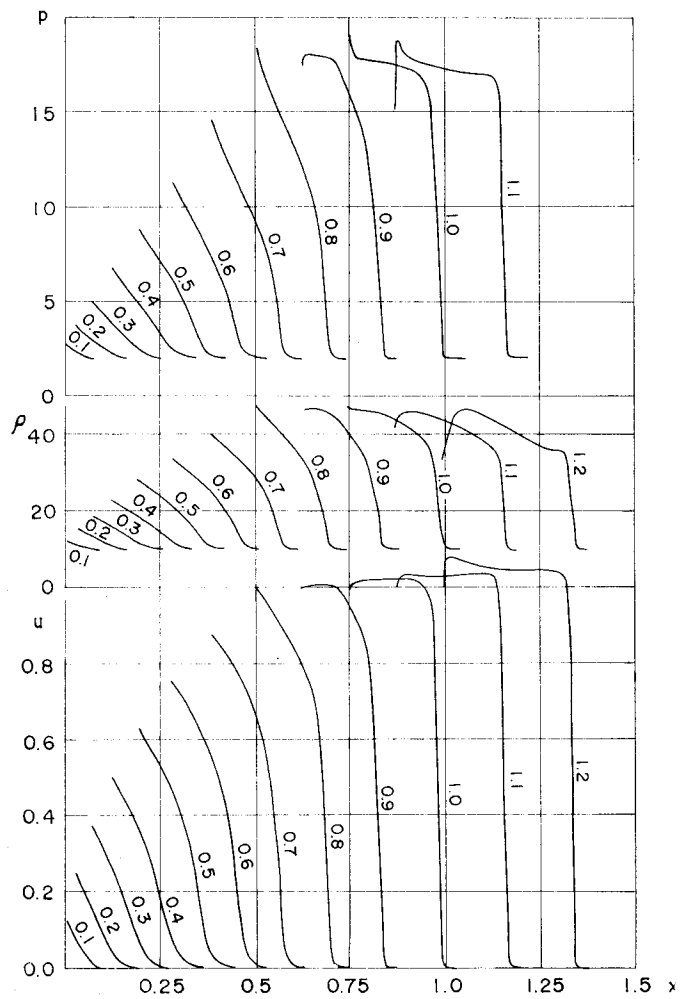


Fig. 20. Method-3.

$$\frac{p'_+ + p_+}{2} = \bar{p}_+ \quad (\text{see (4.1)})$$

$$\frac{\rho'_+ + \rho_+}{2} = \bar{\rho}_+$$

where the prime means the values at A.

The result by this method is shown in the Fig. 20. The calculation overflowed and stopped half way.

(iv) Method-4 This method also is that of §2. But we put

$$p'_+ = p_+ \quad (\text{see (4.1)})$$

$$\rho'_+ = \rho_+$$

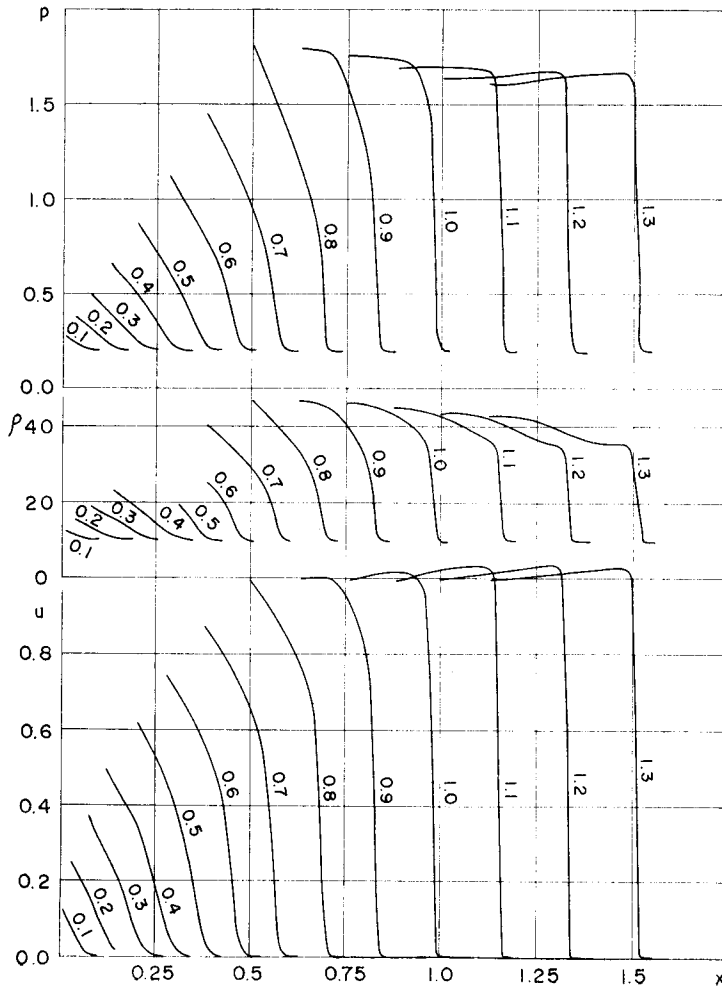


Fig. 21. Method-4,

Its results is shown in the Fig. 21.

This result is best.

(v) Method-5 In addition we shall report the calculation in which the Lax-Wendroff's viscosity method⁴⁾ in the interior region. First in the neighbourhood of the piston we use the same method as Method-1. The result is shown in the Fig. 22.

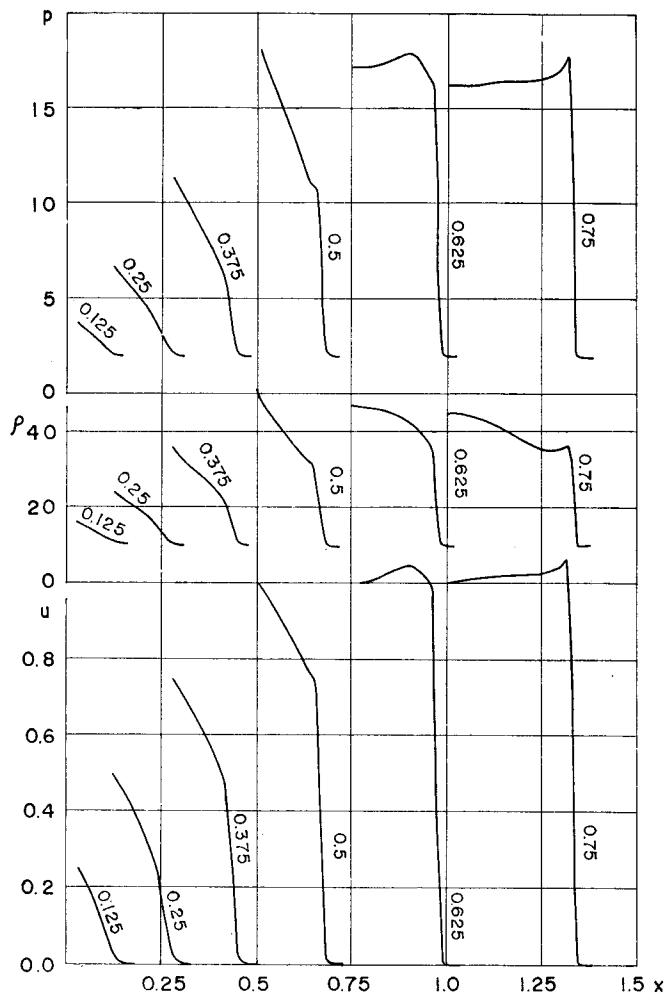


Fig. 22. Method-5.

(vi) Method-6 As above we use the L-W's method. But in the neighbourhood of the piston we use the same method as Method-2.

The result is shown in the Fig. 23,

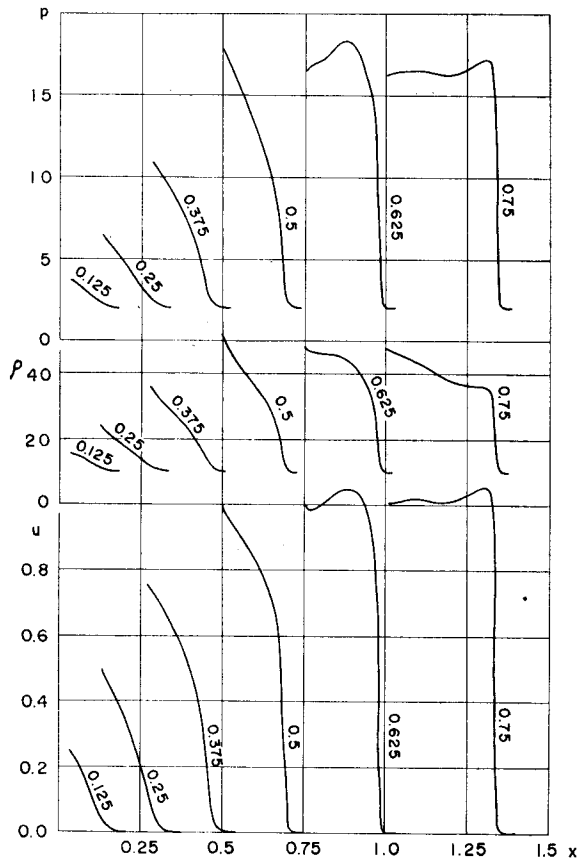


Fig. 23. Method-6.

Appendix III So far we considered the problem in the Eulerian form, but we can treat it also in the Lagrangian form. In this case the fundamental equations are

$$\begin{cases} \frac{\partial V}{\partial t} = \frac{\partial u}{\partial q} \\ \frac{\partial u}{\partial t} = -\frac{\partial p}{\partial q} \\ \frac{\partial \left(e + \frac{u^2}{2} \right)}{\partial t} = -\frac{\partial pu}{\partial q} \\ \left(q = \int \rho dx \quad \frac{\partial x}{\partial t} = u \right) \end{cases}$$

Here q is the Lagrangian coordinate and V is the specific volume ($= \frac{1}{\rho}$). The other values are defined as in §2.

The equation of piston motion is given as follows:

$$\frac{du}{dt} = p(t, -0) - p(t, +0), \quad \text{at } q=0.$$

We shall show the result in which the practical problem of §6 was solved by the exact Godunov's method. (see §3, in detail see 4)). The calculation method in the neighbourhoods of the piston and the wall is analogous to that in §§4, 5. In this calculation the mesh width Δq in the left region to the piston is 0.7897 and that in the right is 0.4387. The time interval Δt is 0.02.

The piston path and the pressure history at the wall are shown in Fig. 6 and Fig. 7 respectively by the broken lines. This result seems to be closer to the experimental one³⁾ than our result by the Eulerian form. But this comparison is not fair since the above mesh width Δq corresponds to the finer Δx .

Acknowledgements

I should like to thank my teacher M. Yamaguti who gave me encouragement continually. I am also grateful to M. Koshikawa who helped me to make the program for the problem in the Lagrangian form. I am indebted to A. Daishoji, who typed my manuscript.

References

- 1) Courant, K. and Friedrichs, K.O., Supersonic flow and shock waves, Interscience Publishers, Inc., 1948.
- 2) Stalker, R. J. A Study of the Free-Piston shock tunnel AIAA Journal, Vol. 5, No. 12 1967.
- 3) Kimura, T. Studies on Hypersonic Gun Tunnel Ph. D. Theses, Kyoto University, 1967.
- 4) Годунов, С. К., Разностный метод численного расчета разрывных решений гидродинамики, Мат. Сбор. Т. 47 (89), No. 3, 1959.
- 5) Lax, R. D. and Wendroff, B. Systems of conservation laws. Comm. Pure Appl. Math., Vol. 13, 1960.
- 6) Годунов, С. К., Забродин, А. В. and Проков, Г. П., Разностная схема для двумерных нестационарных задач газовой динамики и расчет обтекания с отходящей ударной волной, Выч. мат. и мат. физ., Т. 1, No. 6, 1964.
- 7) Richtmyer, R. D. and Morton, K. W., Difference methods for Initial Value Problems. Wiley (Interscience). New York 1967.
- 8) Nogi, T. Difference schemes for the equation of the onedimensional fluid dynamics., Lecture notes at the Institute of the Mathematical Science of Kyoto University, 32, 1967, 10. (in Japanese)